

A Pivotal Role of Cyclic AMP-Responsive Element Binding Protein in Tumor Progression

Rinat Abramovitch,^{1,2} Einat Tavor,³ Jasmine Jacob-Hirsch,⁵ Evelyne Zeira,¹ Ninette Amariglio,⁵ Orit Pappo,⁴ Gideon Rechavi,^{5,6} Eithan Galun,¹ and Alik Honigman³

¹Goldyne Savad Institute of Gene Therapy, ²MRI/MRS Lab, HBRC, ³Department of Virology, and ⁴Department of Pathology, The Hebrew University-Hadassah Medical School, Jerusalem, Israel, and ⁵Department of Pediatric Hemato-Oncology, Safra Children's Hospital, Sheba Medical Center and ⁶Sackler School of Medicine, Tel Aviv University, Tel Aviv, Israel

ABSTRACT

Tumor microenvironment controls the selection of malignant cells capable of surviving in stressful and hypoxic conditions. The transcription factor, cyclic AMP-responsive element binding (CREB) protein, activated by multiple extracellular signals, modulates cellular response by regulating the expression of a multitude of genes. Previously, we have demonstrated that two cysteine residues, at the DNA binding domain of CREB, mediate activation of CREB-dependent gene expression at normoxia and hypoxia. The construction of a dominant-positive CREB mutant, insensitive to hypoxia cue (substitution of two cysteine residues at position 300 and 310 with serine in the DNA binding domain) and of a dominant negative CREB mutant (addition of a mutation in serine¹³³), enabled a direct assessment, *in vitro* and *in vivo*, of the role of CREB in tumor progression. In this work, we demonstrate both *in vitro* and *in vivo* that CREB controls hepatocellular carcinoma growth, supports angiogenesis, and renders resistance to apoptosis. Along with the identification, by DNA microarray, of the CREB-regulated genes in normoxia and hypoxia, this work demonstrates for the first time that in parallel to other hypoxia responsive mechanisms, CREB plays an important role in hepatocellular carcinoma tumor progression.

INTRODUCTION

Cyclic AMP responsive element-binding (CREB) protein is an important transcription factor activated by multiple signal transduction pathways in response to external stimuli, including synaptic activity, hormones, growth factors, cytokines, and stress. Two independent, well-conserved regions mediate activation by CREB: (a) the kinase-inducible domain, which contains a serine residue within a consensus phosphorylation site at position 133 (1, 2), and (b) a basic leucine-zipper domain that governs the binding efficiency of CREB to its cognate promoter element CRE, a consensus palindromic sequence, TGACGTC (Fig. 1A and Refs. 3–6). CREB binds to CRE as a homodimer or heterodimer (7). It was demonstrated that Ser¹³³ phosphorylation has no discernible effect on CREB DNA binding (8–10). The CREB-binding protein, CBP (11), is recruited selectively to phosphorylated CREB to facilitate transcription activation (4). In response to different signals, a number of kinases are involved in phosphorylation of the Ser¹³³ such as protein kinase A (12, 13), Ca²⁺-calmodulin kinases II and IV (14), and the growth factor ras-dependent RSK2 (15).

Although the various signaling pathways converge to CREB, resulting in CREB-mediated activation of gene expression, it is obvious that specific external stimuli should activate a designated repertoire of

genes (for a detailed review, see Ref. 16). Previously, we have demonstrated that under reduced conditions, CREB binds more efficiently to its cognate DNA binding site and increases gene expression at hypoxia relatively to normoxia. This effect is probably independent of phosphorylation of CREB because we did not detect a significant change in the ratio between phosphorylated and nonphosphorylated CREB (3). Moreover, we demonstrated by biochemical and genetic experiments that the redox state of two Cys residues, Cys³⁰⁰ and Cys³¹⁰, determines the efficiency of CREB-mediated transcription activation (3). Thus, CREB protein has an intrinsic mechanism of sensing oxygen concentrations in the cell, leading to changes in the expression level of CREB-regulated genes.

In response to hypoxia, significant biological processes including cell proliferation, angiogenesis, metabolism, apoptosis, and immortalization, undergo meaningful modifications. It is well documented that in different cell lineages, CREB mediates expression of a variety of hypoxia-responsive genes, including the vascular endothelial growth factor (17), lactate dehydrogenase, *LDH1* (3, 18), and the antiapoptotic genes such as *IAP2* (19) and *Bcl2* (20).

Several studies have revealed a role for the CREB family of activators in the control of cell survival and proliferation (21, 22). It has been demonstrated that CREB DNA binding activity and phosphorylation are necessary for the nerve growth factor (NGF)-dependent survival of neurons (23, 24). Several cell cycle genes such as *cyclinD1* and *cyclin A* are regulated by CREB via a functional CRE element (25–27). Microarray analysis of PC3M cells treated with CRE decoy oligodeoxynucleotide (ODN) revealed that many genes related to tumor growth are regulated by the CREB family of transcription factors (28, 29).

Alterations of CRE binding proteins with loss of CREB expression were observed in the human adrenocortical cancer cell line H295R. Similar alterations were found in human malignant adrenocortical tumors (30, 31). Additionally, the involvement of CREB in the control of tumor metastasis was demonstrated in cases of melanoma cells (32, 33). Thus, it appears that various alterations leading to activation or inactivation of key components of the cAMP signaling pathway can be observed in tumorigenesis. In addition, it has been demonstrated that CREB plays an important role in promoting proliferation and cellular adaptive responses (34). Taken together with our previous results that demonstrated increased CREB activity in cells subjected to hypoxia (3), it was suggested that CREB might also play a role in tumor progression. We generated several CREB mutants: the dominant positive CREB300/310 (double Cys to Ser substitution at position 300 and 310) and the dominant negative CREB300/310/133 mutated in addition in Ser¹³³. By using these CREB mutants, we demonstrate *in vivo* and *in vitro* that CREB plays a major role in hepatocellular carcinoma (HCC) tumor progression.

MATERIALS AND METHODS

Plasmids and Cells. All of the cell lines were cultivated in DMEM supplemented with 10% FCS. We used the murine HCC cell line, BNL1ME A.7R.1 (American Type Culture Collection, Manassas, VA), which was orig-

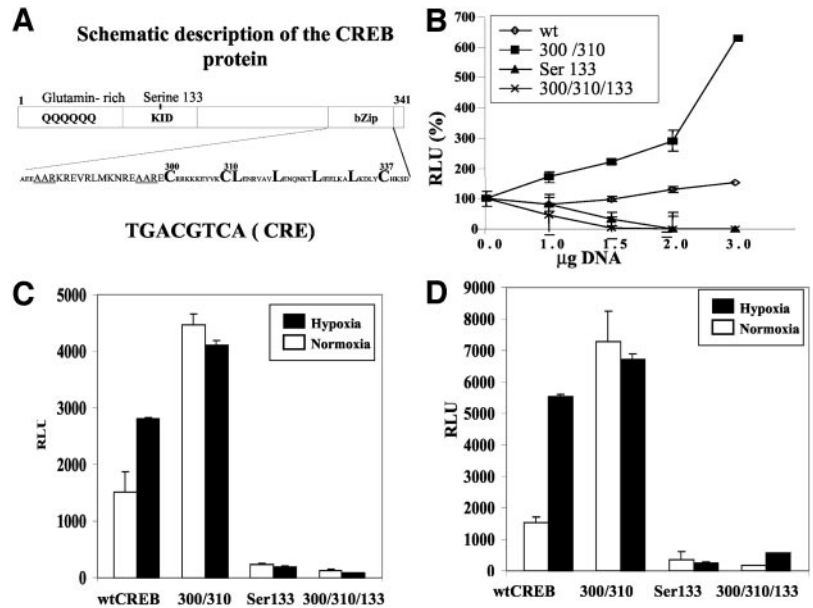
Received 7/14/03; revised 11/24/03; accepted 12/16/03.

Grant support: Ministry of Science and Cultures, Neidersachsen State, Germany (to A. Honigman), in part by the Philip Morris Incorporated fellowship program (to R. Abramovitch), the Horwitz Foundation for Complexity Science (to R. Abramovitch), and the Genetic Therapy Strategic Center supported by the Israeli Ministry of Science.

The costs of publication of this article were defrayed in part by the payment of page charges. This article must therefore be hereby marked *advertisement* in accordance with 18 U.S.C. Section 1734 solely to indicate this fact.

Requests for reprints: Alik Honigman, Virology, Hebrew University-Hadassah Medical School, P. O. Box 12272, Jerusalem 91120, Israel. Phone: 972-2-6758645; Fax: 972-2-6757046; E-mail: Honigman@ml.huji.ac.il.

Fig. 1. A, schematic description of the cyclic AMP responsive element binding (CREB) protein. The glutamine-rich (QQQQQ), the kinase-inducible domain (KID), and the basic leucine-zipper (bZip) domains are indicated. The protein sequence of the bZip domain, emphasizing the Cys residues, Cys³⁰⁰ and Cys³¹⁰, in the basic region as well as serine 133 (Ser¹³³) in the KID domain are depicted. The CRE palindromic sequence is indicated at the bottom. B, effect of CREB variants on CRE-mediated gene expression: HEK293 cells were transfected with increasing amounts of plasmid DNA (abscissa) expressing either wild-type CREB, CREB300/310, CREB M, mutated in Ser¹³³, or the triple mutant CREB300/310/133, together with plasmid pGLCRE expressing the *luc* gene mediated by CRE. Light emission was monitored 48 h later. The relative light emission is expressed as RLUs (relative light units). SD is indicated; $P < 0.02$ compared with wild type. C, effect of hypoxia on CREB-mediated Luc activity: c4HIF^{+/+} cells were transfected as above using 3 μ g of DNA of each CREB-expressing vector. Thirty-two h after transfection, the cells were incubated for an additional 16 h at either normoxia or hypoxia. Light emission in all experiments was normalized to Renilla luciferase activity. SD is indicated; $P < 0.001$ compared with wild type at normoxia. D, effect of CREB-mediated Luc activity in c4HIF^{-/-} cells. Cells were transfected, incubated, and assayed as above. Light emission in all experiments was normalized to Renilla luciferase activity. SD is indicated. $P < 0.007$ compared with wild type at normoxia.



inally established from a BALB/c mouse for the preparation of stable *luc*-expressing tumor cells. These cells were infected with recombinant rLNC/*luc* retroviruses (35), and stable clones were selected by G418 (400 μ g/ml), generating stable infected BNL1ME clones. The cells were additionally cotransfected with a plasmid vector expressing the puramycin resistance gene (pBABE) and any one of the CREB-expressing vectors: pCREBwt; pCREB300/310 (3); pCREB133; and pCREB300/310/133. pCREB133 and pCREB300/310/133 were constructed by replacing the DNA fragment (*Stu*I to *Kpn*I) of either wild-type CREB or the CREB300/310 with the same DNA fragment with a Ser¹³³ to Ala substitution from the pRSVCREB (a kind gift from Dr. Mark Montminy, Stanford University, Stanford, CA). Stable mouse c4 HCC clones (B13Nbi1, Atcc, and CRL-2717) and c4 deleted for the hypoxia-inducible factor (HIF) gene (c4HIF^{+/+} and c4HIF^{-/-}, a kind gift from Dr. Eli Keshet, Hebrew University, Jerusalem, Israel), transfected with the four CREB variants, were selected by G418 after cotransfection with a Neomycin-resistance plasmid.

Luciferase Assay. CRE-mediated luciferase expression was determined using the following cell lines: HEK293; BNL1ME; c4HIF^{+/+}; and c4HIF^{-/-}. These cell lines were transiently cotransfected with CREB-expressing vectors, pGLCRE (3) harboring an artificial cellular somatostatin CRE mediating the *luc* gene expression, and pRL (Promega Corp.) expressing the Renilla *luc* gene controlled by the cytomegalovirus promoter. The latter plasmid was used as an internal control for transfection efficiency. Light emission was monitored 48 h after transfection. The cells were harvested into Passive lysis buffer (Promega Corp.) and monitored by an automatic Anthos Lucy1 photoluminometer (36). The relative light units for CREB-mediated luciferase activity were calculated in all of the experiments by comparison to the activity of Renilla luciferase mediated by the CREB-nonresponsive cytomegalovirus promoter after subtraction of firefly luciferase background activity in cells not transfected with the CREB-expressing vectors.

Growth of Tumor Cells in Soft Agar. BNL1ME cells (3×10^3 and 5×10^3) were sowed into 0.3% Seaplaque Agarose prepared in DMEM and 10% FCS. Every 3 days, fresh medium was added to the plates. The number and size of the colonies were scored periodically under a microscope.

Preparation of cRNA and Gene Chip Hybridization. Total RNA was extracted according to the manufacturing instructions, using SV total RNA purification kit (Promega Corp.). Preparation of cRNA, hybridization, and scanning of the high-density oligonucleotide microarrays [MG_U74A arrays include 12,000 probe sets, which represent all sequences in the Mouse UniGene database (Build 74) that have been functionally characterized (~6,000) and ~6,000 expressed sequence tag clusters; Affymetrix, Santa Clara, CA] were performed according to the manufacturer's protocol (37).

Data Analysis. Microarray Analysis Suite 5. (MAS 5.0; Affymetrix) was used to analyze the data. The expression analysis files created by Genechip 5.0

software were then transferred to a database (Microsoft Access; Microsoft, Redmond, WA) for data filtering. To ensure that the data are reliable, genes were considered to be differentially expressed if P was < 0.025 and fold change was > 2 (Affymetrix Technical Note 2). Cluster analysis was done using Gene Cluster and Treeview programs (38).

Real-Time Quantitative Reverse Transcription-PCR. RNA was extracted as described above, and cDNA was synthesized using the Reverse-iT first strand synthesis kit (Abgene) according to the manufacturer's instructions. In addition to the Cyr61- (GenBank accession no. Mm00487498) and β -2 microglobulin (GenBank accession no. NM_009735)-specific primers, fluorogenic Taqman probes were used (Assay on demand gene expression system; Applied Biosystems). The housekeeping gene sequence β -2 microglobulin (GenBank accession no. NM_009735) was chosen as a control because this gene was not affected by CREB or hypoxia in the DNA microarray analysis. Real-time quantitative PCRs (45 cycles) were performed on the ABI Prism 7900HT platform in a total volume of 20 μ l, according to manufacturer instructions.

Animal Protocol. BALB/C mice (6 weeks old, 20-g body weight) were implanted s.c. in the lower back with 10^6 BNL1ME HCC cells stably transfected with the *luc* gene and one of the CREB variants: wild-type CREB; CREB300/310; and CREB300/310/133. The Hebrew University Animal Care Committee approved all of the animal experiments.

In Vivo Luciferase-Based Imaging of Gene Expression. For continuous detection and quantification of gene expression in the live animals, we used the cooled charge-coupled device imaging system, as described previously (35). In brief, we used the Roper Chemiluminescence Imaging System, which contains the cooled charge-coupled device model LN/CCD-1300EB equipped with ST-133 controller and a 50-mm Nikon lens (Roper Scientific, Princeton Instrument, Trenton, NJ). In all experiments, the mice were anesthetized before light detection, and 5 min before monitoring light emission, they were injected i.p. with Beetle luciferin (Promega Corp., Madison, WI) in PBS at 126 mg/kg body weight. The animals were placed in a dark box provided with a controlled light. The light measurements were taken under identical conditions, including exposure time (2 min) and distance of lenses from the mice.

Magnetic Resonance Imaging (MRI) Analysis of Tumor Volume and Blood Vessel Density, and Functionality. MRI experiments were performed on a horizontal 4.7-T Biospec spectrometer (Bruker Medical, Ettlingen, Germany), with an active radio frequency-decoupled surface coil 2 cm in diameter (39). Mice (7 mice of each of the previously described groups) were anesthetized (pentobarbital; 30 mg/kg i.p.) and placed supine, with the tumor located at the center of the surface coil. For analysis of tumor growth, coronal and axial gradient echo images were acquired. Tumor vascularization was reflected by reduction of the mean signal intensity around the tumor in gradient echo T_2^* -weighted images (repetition time/echo time = 100/10 ms; field of

view = 4 cm; 256 × 256 pixels; in plane resolution = 150 μm and slice thickness of 0.6 mm). Data are reported as the apparent vessel density [AVD = $-\ln(s(t)/s(0))$] in which $s(t)$ is the mean intensity in a 1-mm region surrounding the tumor, and $s(0)$ is the mean intensity of a distant muscle, as described previously (39, 40). Tumor vessel functionality was determined from gradient echo images acquired during the inhalation of air-CO₂ and carbogen as described previously (40). Four images were acquired at each gas mixture (51 s/image; slice thickness = 1 mm; repetition time/echo time = 100/10 ms; field of view = 3 cm; 256 × 128 pixels; in plane resolution = 110 μm; four averages). Other experimental details were as reported previously (39, 40).

Data Analysis. MRI data were analyzed using IDL software (Research Systems, Inc.). Vascular function was derived from images acquired during inhalation of carbogen and air-CO₂ using the equation described in previous studies (39, 40). Vessel functionality measures the capacity of erythrocytes to deliver oxygen from the lungs to each pixel in the image (39). Mean vessel functionality values were calculated from the entire tumor and were divided by the mean values from a region with the same size taken at the contra lateral side.

Histology. Tissue samples were fixed in 4% formaldehyde in PBS, embedded in paraffin, and sectioned (5-μm sections). After deparaffinization and rehydration, sections were washed (three times) with PBS and stained with H&E.



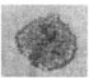
Determination of Microvessel Density, Proliferative Activity, and Apoptosis. Blood vessels were detected by staining with anti-factor VIII antibody (von Willebrand factor; Dako). The anti-von Willebrand factor antibody was used in a 1:150 dilution after trypsinization for 30 min at 37°C. The number of blood vessels was counted in 10 randomly selected fields (magnification, ×400) of each tumor. Proliferation index was determined on histological sections of the various tumors and analyzed by a professional pathologist blindly. The number of mitoses were counted in ten randomly selected fields (magnification, ×400) of each tumor. For apoptosis analysis, 5-μm thick sections of tumor tissue were processed and stained with the DeadEnd Fluorometric TUNEL System (Promega Corp.) according to the manufacturer's protocol and counterstained with propidium iodide. Apoptotic cells were counted using confocal microscope (magnification, ×400). A total of 10 fields/tumor was analyzed, and the mean value ± SD was determined. All these results were subjected to statistical student *t* test analysis.

RESULTS

Activation of Gene Expression by CREB Variants. Previously, we have demonstrated that conversion of the two Cys residues at position 300 and 310 to Ser (CREB300/310; Fig. 1A) enhanced CREB binding efficiency and CREB-mediated gene expression (Fig. 1; Ref. 3). A mutation in Ser¹³³ results in inactivation of CREB transcriptional activity (12). By converting the Ser¹³³ into Ala in the CREB300/310, we expected to generate a strong negative dominant CREB mutant (CREB300/310/133). To test the effect of these CREB variants on CRE-mediated gene expression, HEK293 cells were transfected with plasmids expressing the three CREB variants, together with the reporter plasmid pGLCRE (3), expressing the *luc* gene from a CRE-dependent promoter. Luc activity was determined in crude extracts 48 h after transfection. The results presented in Fig. 1B clearly demonstrate that relative to the wild-type CREB, CREB300/310 enhances luciferase gene expression up to 6-fold in a dose-response manner ($P < 0.002$), whereas CREB133 and CREB300/310/133 abolish CREB-mediated luciferase expression ($P < 0.002$). To elucidate the effect of HIF-1 on CREB-mediated gene expression, c4HIF^{+/+} and c4HIF^{-/-} cells were transfected as above and incubated either at normoxia or at hypoxia conditions for 16 h. The results, presented in Fig. 1, C and D, demonstrate that the activity of Luc induced by wild-type CREB at hypoxia increased by ~2- and 3-fold in HIF^{+/+} and HIF^{-/-} cells, respectively, relative to normoxia ($P < 0.001$), whereas CREB300/310 gene activation was not affected by hypoxia. CREB133 and, especially the triple CREB mutant CREB300/310/133, abolished CRE-dependent luciferase expression

Table 1 Growth of cyclic AMP-responsive element binding (CREB)-transfected cells in soft agar

BNL1ME cells stably transfected with plasmids expressing any one of the specified CREB variants (first column) were sowed into soft agar. Pictures of the colonies were taken under microscope (magnification, ×200); a typical colony is presented, the size was measured and the volume of the colony was determined. The volume of an average colony is presented. The numbers of colonies in each plate were counted, and the percentage of colony forming cells was calculated relative to the number of sowed cells. The results represent an average from several experiments; the SD and *P* compared with wild type are indicated.

CREB variants	Typical colony	Representative volume in cm ³	Colony growth (%)
Wild type		0.03	6.2 ± 6
Cys300/310		0.17	14.4 ± 3 p = 0.05
Cys300/310/133		0.013	0.76 ± 0.6 p = 0.08

dramatically, competing out the genomic-encoded CREB ($P = 0.02$). Similar results were obtained with CREB-deficient F9 cells (3) HEK293 and HCC BNL1ME cells transfected with the various CREB mutants (results not shown).

Effects of CREB Mutants on HCC Growth *In Vitro*. The ability of cells to grow in soft agar is a commonly used assay for transformed cells. The effect of CREB mutants on BNL1ME growth characteristics *in vitro* was tested in soft agar plates. BNL1ME pools of clones, stably expressing each of the CREB variants, wild-type CREB, CREB300/310, and CREB300/310/133 cells (3×10^3 and 5×10^3), were sowed into soft agar. Cells expressing the CREB300/310 grew much faster than the control cells expressing the wild-type CREB. They formed an increased number (14.4% of the inoculated cells compared with 6% of the wild-type CREB) of larger and more defined colonies within 14 days (Table 1). Wild-type CREB stable transfected cells developed into relatively smaller and less defined colonies. The cells expressing CREB300/310/133 hardly developed colonies in soft agar (0.76%). Those that did grow developed very poorly into non-defined small colonies (Table 1). It should be noted that we could not detect any effect on the growth rate of the stable clones expressing the various CREB mutants when cultivated *in vitro* (not in soft agar).

DNA Array Analysis of CREB-Mediated Gene Expression in Response to Hypoxia. We demonstrated above that CREB 300/310 enhances CREB activity at normoxia similar to the wild-type CREB at hypoxia. We expected that comparison of gene expression patterns mediated by CREB300/310 at normoxia and wild-type CREB at hypoxia to gene expression in cells harboring wild-type CREB at normoxia would help us to identify the CREB-mediated cellular genes at hypoxia, independently of HIF activation. DNA-array expression analysis comparing CREB300/310 dominant positive mutant to wild-type CREB was performed with RNA purified from the BNL1ME stable clones incubated at either normoxia or hypoxia. The cDNA was used to probe a mouse DNA chip (37) that represents 12,000 genes (Fig. 2). Only genes whose expression changed in at least 2-fold magnitude were clustered using the EISEN clustering program (38).⁷

As can be seen in Fig. 2A, the expression of 77 genes was clearly affected by CREB, either up- or down-regulated (Table 2), when stringent criteria were applied. These genes are common to the set of

⁷ Internet address: <http://rana.lbl.gov/EisenSoftware.htm>.

Fig. 2. DNA array analysis of cyclic AMP responsive element binding (CREB)-regulated genes. A, schematic description of the analysis of the DNA array experimental results. RNAs purified from BNL1ME cells expressing either wild-type CREB (wt) or CREB300/310 (mut) at normoxia (N) or hypoxia (H), were analyzed by Affymetrix mouse DNA arrays. The CREB-regulated genes were determined by defining the genes with altered expression (>2 -fold) common to CREB300/310 at normoxia versus (v) wild-type CREB at normoxia and wild-type CREB at hypoxia versus normoxia. The effect of hypoxia on gene expression was determined by the change in gene expression in cells harboring CREB wt or CREB300/310 at hypoxia relative to cells expressing wild-type CREB at normoxia. B, genes (2191) that changed by at least 2-fold were subjected to the Eisen clustering program analysis.⁷ Normoxia (right side cluster); 1-N(wt), 2-N(mut), and hypoxia (left side cluster); 3-H(wt), 4-H(mut). The genes colored in green are down-regulated, and the red colored are up-regulated as compared with the geometric mean (geomean) value. C, functional analysis of genes affected by hypoxia.

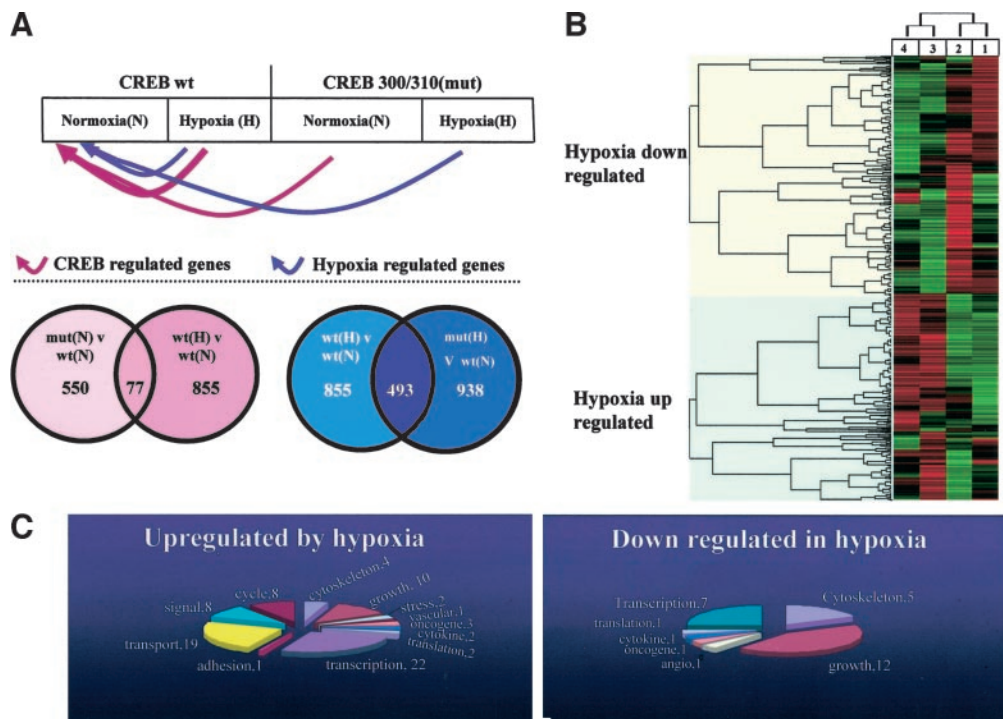


Table 2 Genes regulated by wild-type cyclic AMP-responsive element binding (CREB) at hypoxia and by CREB300/310 at normoxia

The CREB-regulated genes are arranged according to the fold of change (≥ 2.1 with a $P \leq 0.0025$) induced by CREB300/310 (m) at normoxia (N) relative to wild-type CREB (wt) at normoxia (N). The effect of hypoxia on wild-type CREB-mediated genes was determined by comparison of gene expression at hypoxia to normoxia (Hwt/Nwt).

AffyID	Accession no.	Symbol	Name	Nmt/Nwt	Hwt/Nwt
Up-regulated by CREB					
92830_s_at	X14678	Zfp36	Zinc finger protein 36	11.3	9.8
101857_at	AB006036	Srpk2	Serine/arginine-rich protein-specific kinase 2	8	6.1
160618_at	AA760613	Lgals8	Lectin, galactose binding, soluble 8	7	3
99350_at	C76102	Sec63	SEC63 (<i>S. cerevisiae</i>)	5.7	5.7
103061_at	Z49976	Gad1	Glutamic acid decarboxylase 1	4.9	2.3
103006_at	AB012276	Atf5	Activating transcription factor 5	4.3	5.7
96869_at	AW124839	Gabarap	γ -aminobutyric acid receptor-associated protein	4	2
104669_at	U73037	Irf7	IFN regulatory factor 7	3.5	2.1
102696_s_at	A1747899	Pitpnb	Phosphatidylinositol transfer protein, β	3.2	2
102737_at	U35233	Edn1	Endothelin 1	3.2	2.6
103578_at	AJ006972	Tom1	Target of myb1 homologue (chicken)	2.8	4.6
103957_at	X57349	Trfr	Transferring receptor	2.8	2.5
92777_at	M32490	Cyr61	Cysteine rich protein 61	2.6	2
98104_at	A1842889	Atp6f	ATPase, H ⁺ transporting, lysosomal (vacuolar proton pump)	2.6	2.3
101947_at	AB028921	Nakap95-pending	Neighbor of A-kinase anchoring protein 95	2.6	3.2
160119_at	A1845538	Etv6	Ets variant gene 6 (TEL oncogene)	2.5	7
94918_at	A1839392	C76919	Expressed sequence C76919	2.3	3.2
97859_at	AA762325	Nkx6-2	NK6 transcription factor related, locus 2 (<i>Drosophila</i>)	2.3	2.5
96841_at	AW046627		Serine threonine kinase pim3	2.3	2.3
104048_at	A1848732	Cars	Cysteinyl-tRNA synthetase	2.3	8
104598_at	X61940	Ptpn16	Protein tyrosine phosphatase, nonreceptor type 16	2.3	2.5
102292_at	U00937		Cluster Incl U00937:Mus musculus GADD45 protein (gadd45) gene	2.3	4
92603_at	U13840	Atp6d	ATPase, H ⁺ transporting, lysosomal (vacuolar proton pump), 42 kDa	2.1	2.1
95057_at	A1846938	Herpud1	Homocysteine-inducible, endoplasmic reticulum stress-inducible, ubiquitin-like domain member 1	2.1	7
98048_at	AF060490	Nssr	Neural-salient serine/arginine-rich	2.1	3.2
101995_at	U40930	Sqstm1	Sequestosome 1	2.1	3.5
102798_at	U77630	Adm	Adrenomedullin	2.1	3.5
Down-regulated					
96055_at	X59520		Cluster Incl X59520:Cholecystokinin	7	2.1
96585_at	AJ006691		Cluster Incl AJ006691:Mus musculus v2r gene	6.5	3.7
100030_at	D44464	Upp	Uridine phosphorylase	3.5	2
102389_s_at	A1841303	Gap43	Growth associated protein 43	2.8	2.5
93550_at	D88792	Csrp2	Cysteine-rich protein 2	2.6	2
161117_at	AJ243963	Dkk2	Dickkopf2	2.6	12.1
95434_at	AI851740	Arpc3	Actin related protein 2/3 complex, subunit 3 (21 kDa)	2.3	2.5
103556_at	A1840158	AW260363	Expressed sequence AW260363	2.1	8
97934_at	U73820	Galnt1	UDP-N-acetyl- α -D-galactosamine:polypeptide N-acetylgalactosaminyltransferase 1	2.1	2.3
160477_at	AW046205	Ndufa4	NADH dehydrogenase (ubiquinone) 1 α subcomplex, 4	2.1	2.1
160655_at	D85391	Cpd	Carboxypeptidase D	2.1	2.3

genes regulated by the dominant positive CREB mutant compared with the wild-type CREB in normoxia and to the genes regulated by the wild-type CREB in hypoxia compared with normoxia. Using the Gene Ontology Tool of the NetAffx Analysis Center of Affymetrix, 37 annotated genes of the 77 CREB-regulated genes (Table 2) were classified into seven functional groups (Fig. 3).

Many more genes, 493, were designated as hypoxia-regulated genes. These genes are common to the set of genes regulated by hypoxia in the wild-type CREB-transfected cells *versus* the same cells in normoxia and to the genes regulated by hypoxia in the CREB300/310-transfected cells compared with the genes induced in normoxia by wild-type CREB (Fig. 2). Fig. 2C depicts the functional classification of genes regulated by hypoxic conditions. Genes classified as associated with transcription and transport functions constitute the large functional subgroups up-regulated by hypoxia. Genes involved in growth control and transcription represent major functional groups of genes significantly down-regulated by hypoxic conditions.

The HIFs are primarily regulated via a two-step mechanisms of HIF posttranslational modification affecting both stability and transactivation capacity (41, 42). Indeed, neither wild-type CREB nor CREB300/310 affected the levels of HIF-1 RNA at either normoxia or hypoxia.⁸ HIF-2 and HIF-3 mRNAs were not detectable in our experiments.

Confirmation of Array Results Using Real-Time Reverse Transcription-PCR and Effect of HIF-1 and CREB on the Expression of Cyr61. One of the genes that we found to be up-regulated by CREB is Cyr61 (Table 2). It was shown that Cyr61, a member of the Cyr61/CTGF/NOV (CCN) family of genes (43), is hypoxia inducible in malignant melanoma cells controlled by activator protein 1 and HIF-1 α (44). Sequence analysis of the Cyr61 promoter region revealed that in addition to the activator protein 1 consensus box and several HIF-1 α binding sites, an almost complete CRE site GACGTC (missing the first T of the CRE palindrome) is located at position -81 (European Molecular Biology Laboratory GenBank accession no. HSA249826). CRE sites are usually located within 100 bases up-stream of the TATA box. It was previously demonstrated that the CRE site occurs also as a half-site motif (CGTCA), which is still responsive to CREB activation (16). RNA was purified from c4HIF^{+/+} and c4HIF^{-/-} cells, stably transfected with wild-type CREB and CREB300/310, grown at either normoxia or hypoxia. RNA of Cyr61 was quantified by real-time PCR in comparison to RNA of the housekeeping gene β -2 microglobulin. The expression of this gene did not change in the various conditions, either in the DNA microarray experiment or the real-time PCR. The results presented in Fig. 4A indicate that in c4HIF^{+/+} cells, CREB participates in the up-regulation of Cyr61 at both normoxia and hypoxia. The level of Cyr61 RNA increased in the presence of CREB300/310 by 4.5-fold at normoxia or hypoxia, relative to cells harboring wild-type CREB at normoxia. At hypoxia, the level of Cyr61 RNA in cells expressing wild-type CREB increased by ~3.6-fold relative to normoxia (Fig. 1C and Table 2). In c4HIF^{-/-} cells, the level of Cyr61 increased in cells expressing CREB300/310 by ~2.5-fold at normoxia or hypoxia relative to wild-type CREB, indicating that CREB plays a role in the regulation of this gene. However, in accordance with the results of Kunz *et al.* (44), in the absence of HIF, the expression of Cyr61 decreases 2.5-fold in hypoxia relative to normoxia in the presence of either wild-type CREB or CREB300/310.

Effect of CREB Mutants on the Growth of HCC Tumors *in Vivo*. We have demonstrated thus far that CREB activity is enhanced at hypoxia, that this enhanced activity is mimicked by CREB300/310 at normoxia, and that CREB300/310/133 has a dominant negative

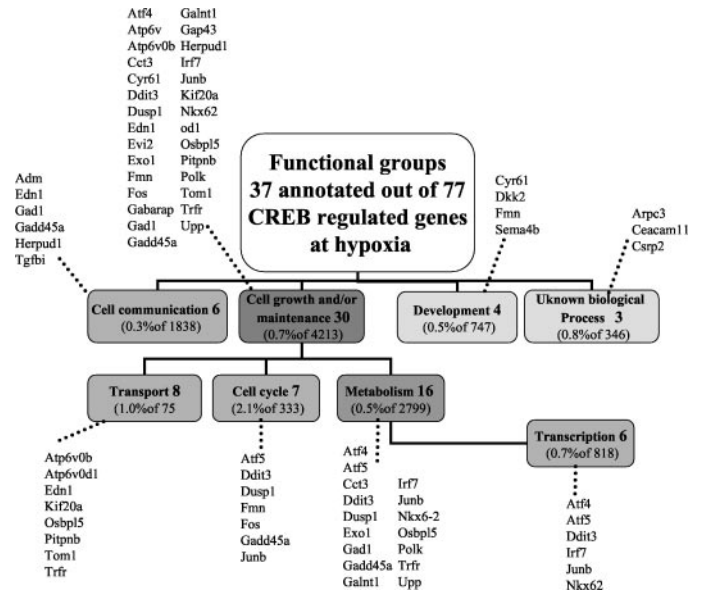


Fig. 3. Functional analysis of cyclic AMP responsive element binding (CREB)-mediated genes at hypoxia. The annotated 37 of the 77 genes whose expression changed by >2-fold, either by CREB300/310 at normoxia or by the wild-type CREB at hypoxia, were diverged into seven functional groups, using the Gene Ontology Tools of the NetAffx Analysis Center.⁹ Some of the genes share more than one functional group.

effect on CRE-mediated gene expression. Taken together with the observation that the mutations in the CREB DNA binding domains alter the growth characteristics of the HCC cell line in soft agar, we hypothesized that CREB may affect growth characteristics of tumors *in vivo*.

To test this hypothesis, Balb/C mice were implanted s.c. with 10⁶ BNL1ME cells stably expressing the *luc* gene and either one of the CREB variants: wild-type CREB; CREB300/310; or CREB300/310/133. Tumor growth kinetics was monitored noninvasively by both light emission recorded by a cooled charge-coupled device camera (Fig. 5, A and B) and by MRI (Fig. 5, C-F). At the end of these experiments, mice were sacrificed and tumor sizes were measured and assessed histologically (Fig. 6 and Table 3). Both noninvasive imaging methods, the cooled charge-coupled device and MRI measurements, demonstrate that CREB300/310 dramatically enhances tumor growth, whereas CREB 300/310/133 inhibits the growth of the implanted tumor cells (Figs. 5 and 6, A-C). Although growth of the wild-type CREB-transfected HCC cells started only 20–23 days after implantation, the CREB300/310 stably transfected cells started growing after 5 days (Fig. 5F). On day 42, the latter tumors were much larger than those expressing the wild-type CREB.

When the HCC cells stably transfected with CREB300/310/133 were implanted, tumors barely grew (Fig. 5). These tumors started to grow only 30 days after implantation and at a slower rate than tumors expressing just the wild-type CREB.

Effects of CREB Variants on Tumor Cell Proliferation and Apoptosis *in Vivo*. Because the CREB300/310 mutation caused enhanced tumor growth, we assessed whether there were differences in the proliferation rate and in tumor cell death. Histological examination of tumor sections taken 34 days after implantation revealed that CREB300/310 mutation enhanced proliferation of HCC cells *in vivo* and reduced apoptosis (Table 3 and Fig. 6, G-L). The number of mitotic cells was significantly higher in the tumors expressing CREB300/310 compared with those expressing wild-type CREB (42 ± 14 *versus* 17 ± 3, respectively, *P* = 0.0003). In addition, there

⁸ Internet address: http://www.hadassah.org.il/departments/Gen_Ther.

⁹ Internet address: <http://www.affymetrix.com>.

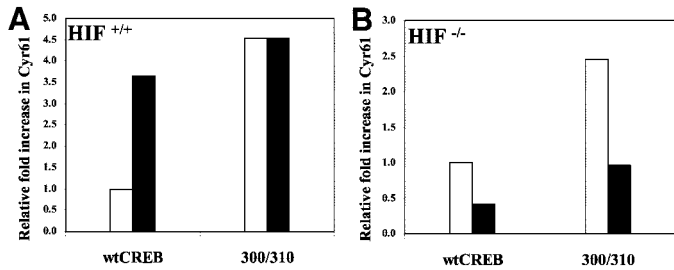


Fig. 4. Real-time quantitative PCR result of the expression of *Cyr61*. RNA extracted from c4HIF^{+/+} (A) and c4HIF^{-/-} (B) stably transfected cells, expressing either one of the two of cyclic AMP responsive element binding (CREB) variants, were analyzed. The cells were incubated for 16 h at normoxia (□) or hypoxia (■). The results at each point were normalized to the values of the housekeeping gene β -2 microglobulin. The results are presented as the folds increase relative to the wild-type CREB at normoxia.

were only few apoptotic cells in CREB300/310 mutated tumors compared with the wild-type tumors (6 ± 2.6 versus 44 ± 20 , respectively, $P = 0.00003$; Table 3 and Fig. 6G–L). The expression of CREB300/310/133 resulted in a decrease in the proliferation index (8 ± 1 , $P = 0.004$), as well as a decrease in the apoptotic index to 2.6 ± 2 , $P = 0.003$.

Effect of CREB Variants on Tumor Vascularization. It was suggested that CREB is involved in hypoxia-induced angiogenesis (through vascular endothelial growth factor regulation; Ref. 17). We therefore assessed the effect of different CREB mutants on tumor vascularization. Indeed, the premature tumor growth of tumors expressing CREB300/310 was accompanied by early and accelerated vascularization toward the tumors, as determined by MRI (Fig. 5G). During the first 3 weeks, the tumor periphery of CREB300/310-transfected tumors was highly vascularized compared with the wild-type CREB transfected tumors (Fig. 6, D–F and Table 3). Subsequently, when tumor growth progressed, the vascularization of both wild-type and CREB300/310-transfected tumors became comparable (Table 3). Up to 3

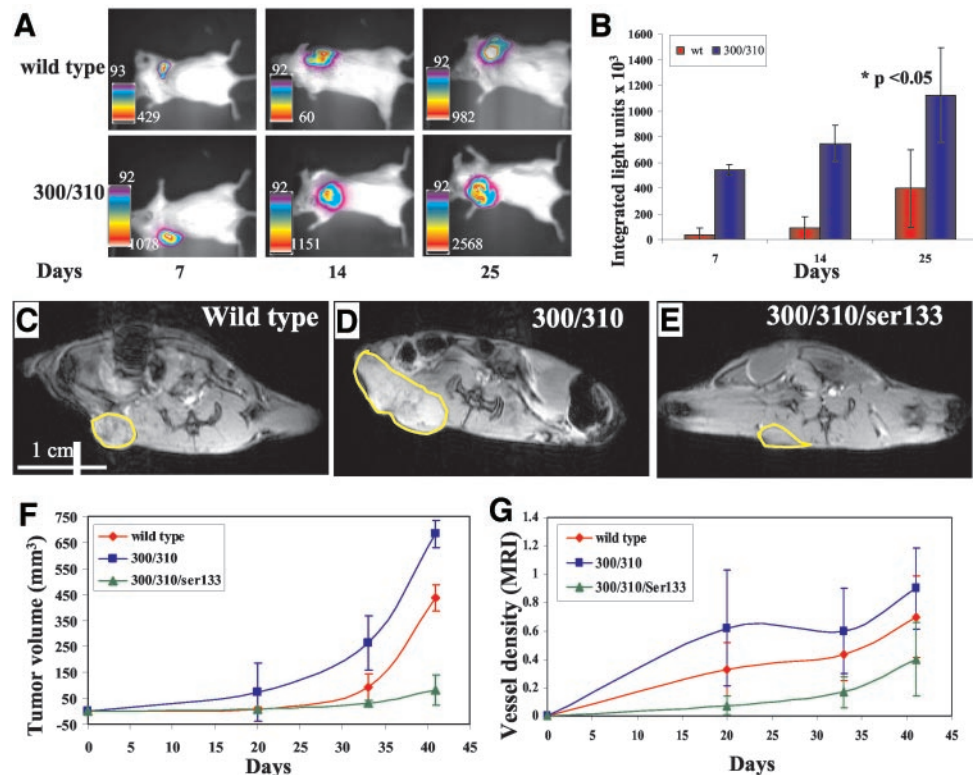
weeks after implantation of tumor cells expressing CREB300/310/133, tumors barely grew, and fewer blood vessels were induced (Figs. 5 and 6 and Table 3). However, on day 34, vascularization rate of the tumors expressing wild-type or CREB300/310/133 became similar to CREB300/310 (Fig. 5G). As a consequence, when comparing whole tumor vascularization (vessel functionality fold), no difference between the wild type (3 ± 1.9) and the CREB300/310 (3 ± 1.7) was observed. This was also confirmed by counting blood vessels on histological sections stained positive for factor VIII (Table 3).

DISCUSSION

Although much knowledge has been accumulated with regard to the mechanisms underlying CREB-mediated activation of gene expression, very little is known of the cellular conditions that may affect the binding of CREB to its cognate DNA binding site. Previously, we have demonstrated that two Cys residues in the basic leucine-zipper domain control the binding efficiency of CREB to CRE and TRE and control of CRE-mediated gene expression in response to redox and hypoxia (3). Thus, CREB may have an intrinsic oxygen-sensing mechanism that enhances CREB activity in cells deprived of oxygen. Although most studies related to response to hypoxia have concentrated on the HIF-1 pathway (41), other transcription factors were shown to be involved in the cellular response to hypoxia, including CREB (42). Here, we demonstrate that genetic manipulation of the cysteine residues at the DNA binding domain of CREB (3) leads to alteration of the cellular response to hypoxia and greatly affects tumor progression via alteration of gene expression.

Hypoxia, a hallmark of many tumors, is associated with angiogenesis and tumor progression. It has been demonstrated that CRE-decoy oligonucleotides inhibit activator proteins 1 and 2 CRE-directed gene transcription *in vivo* and *in vitro*, altering the expression of a variety of cluster genes associated with tumor progression (29, 45). Unlike the experimental setup using the CRE-decoy, which affects all of the

Fig. 5. Monitoring tumor growth and vascularization. A, BNL1ME/Luc (1×10^6) cells, stably transfected with either wild-type of cyclic AMP responsive element binding (CREB; top row) or CREB300/310 (bottom row), were s.c. implanted in BALB/c mice (5–6 weeks old). Light emission from the growing tumors was monitored with the cooled charge-coupled device up to 25 days. The values indicated on the color scale are the maximum and minimum of the gray level. B, graphic presentation of tumor growth as defined by the acquisition of light by the cooled charge-coupled device camera expressed as integrated light/2 min. $P < 0.05$, $n = 4$ /group. Representative transverse gradient echo images of tumors from wild-type CREB-transfected cells (C); CREB300/310-transfected cells (D), and CREB 300/310/133-transfected cells (E), scanned on day 34 after cell implantation. The tumors are circled in yellow, scale bar = 1 cm. F, analysis of the effects of the different CREB mutations on tumor progression was monitored noninvasively using magnetic resonance imaging. Tumor volume was determined from two orthogonal sets of multislice gradient echo images covering the entire tumor on days 20, 34, and 42 after cell implantation ($n = 7$ /group). G, magnetic resonance imaging analysis of vessel density around tumors. Tumor-bearing mice were imaged on days 20, 34, and 42 after cell implantation, as described in "Materials and Methods."



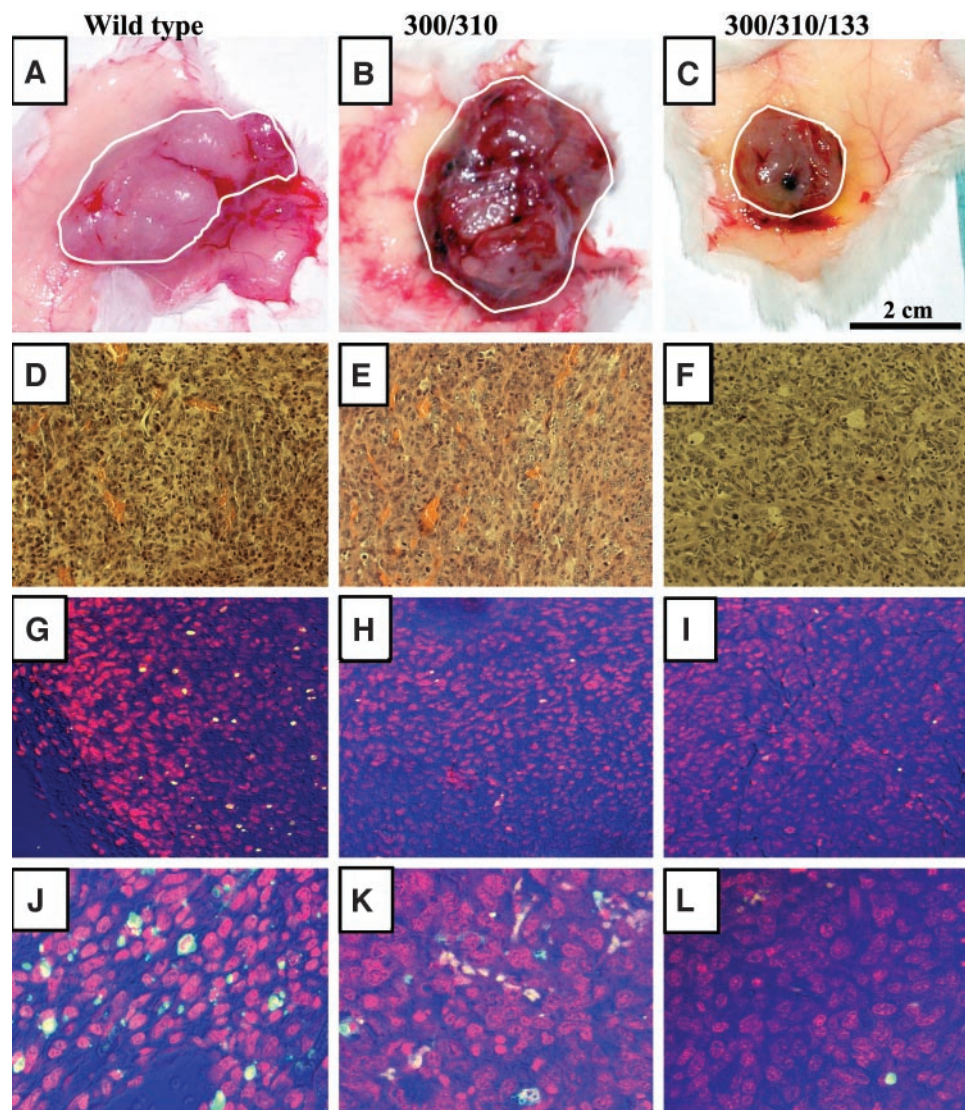


Fig. 6. Histological analysis of vascularization and apoptosis. *A–C*, macroscopic presentation of representative tumors. Tumors (circled in *white*) were excised and photographed on day 34, scale bar = 2 cm. (*D–F*). Histological sections of tumors excised on day 34 and stained with H&E (magnification, $\times 200$). Tumors produced by CREB300/310-expressing cells (*B* and *E*), wild type of cyclic AMP responsive element binding (CREB; *A* and *D*), and CREB 300/310/133 cells (*C* and *F*). Histological sections of tumors dissected on day 34 stained with the DeadEnd Fluorometric TUNEL System (*green*) and counterstained with propidium iodide (*red*; *G–I*). *G–I*, $\times 200$ magnification. *J–L*, $\times 400$ magnification.

CRE binding proteins in this study, including CREB, CREM, ATF, and CREB/Jun heterodimers, we investigated solely the role of CREB in tumor progression by genetic alterations of the CREB DNA binding and the phosphorylation protein domains. We demonstrated that CREB plays a major role in the control of tumor growth and vascularization. Conversion of the two Cys residues at positions 300 and 310 to serine generated a hypoxia-insensitive positive dominant

Table 3 Analysis of histological sections of transfected tumors by the cyclic AMP-responsive element binding (CREB) variants

BNL1ME tumors expressing either one of the specified CREB variants were excised on day 34, and histological sections were microscopically analyzed from random fields (peripheral and central) throughout the whole tumor. Proliferation index figures represent an average number of the cells undergoing division as determined by mitotic nuclei in 10 fields ($\times 100$). The sections were stained for apoptosis (terminal deoxynucleotidyl transferase-mediated nick end labeling) and analyzed under a confocal microscope. The number of fluorescent nuclei was determined in 10 fields ($\times 400$). The numbers represent the average of apoptotic cells/field. Number of vessels/field was determined from sections stained with an antifactor VIII antibody, an average of six fields was monitored for each tumor ($\times 400$). Mean value \pm SD and *P* values are indicated.

CREB variants	Proliferation index	Apoptotic cells/field	Vessels/field
Wild type	17 \pm 3	44 \pm 20	14 \pm 1
300/310	42 \pm 14 (<i>P</i> = 0.0003)	6 \pm 2.6 (<i>P</i> = 0.00003)	16 \pm 12 (<i>P</i> = 0.13)
300/310/133	8 \pm 1 (<i>P</i> = 0.004)	2.6 \pm 2 (<i>P</i> = 0.003)	3 \pm 1 (<i>P</i> = 0.001)

CREB mutant, which alters the kinetics of tumor growth and vascularization (Figs. 5 and 6 and Table 3). The growth and vascularization of tumors stably expressing CREB300/310 precedes the growth and vascularization of tumors transfected with the wild-type CREB by ~ 15 days (Fig. 5). The enhanced growth of tumors expressing the CREB300/310 was accompanied with a higher mitotic index and abrogated apoptosis (Table 3). These changes may contribute to enhanced tumor growth. Abrogation of apoptosis is in agreement with the findings that CREB controls the expression of the antiapoptotic genes IAP2 (19) and *BclIII* (20). Conversion of Ser¹³³ to alanine at the CREB phosphorylation domain in CREB300/310 generated a negative dominant mutant (CREB300/310/133), which abrogates the growth and vascularization of the HCC tumors (Figs. 5 and 6). Only few apoptotic cells were found in these tumors (Table 3 and Fig. 6, *I–L*). The diminished number of apoptotic cells in CREB300/310/133 might be due to smaller tumor size. It is possible that the cells in such a small tumor do not suffer from hypoxia.

Histological analysis of the various tumors on day 34 after implantation demonstrates that CREB300/310 tumors are less necrotic than those expressing the wild-type CREB (data not shown).

On day 46 after implantation of the tumor cells, no significant difference was observed in size and vascularization of the wild-type or CREB 300/310 tumors. This might be explained by our finding that

under hypoxia, activation of CREB-mediated gene expression is similar to that of CREB300/310 at normoxia.

DNA microarray analysis of BNL1ME HCC or cell clones expressing either the wild-type CREB or CREB300/310 suggests that the effect of CREB on promotion of tumor cell proliferation, inhibition of apoptosis, and enhancement of angiogenesis is associated with a prominent change in CREB-mediated gene expression in response to hypoxia. Many of the genes found in the selected cluster of CREB-induced genes are known to mediate those functions. The role of some of these genes is discussed.

Endothelin-1, a potent vasoconstrictor peptide, which was recently shown to be a mitogen that protects cells from apoptosis, induces angiogenesis, and promotes tumor progression and metastasis (46), is greatly induced by CREB and by hypoxia (Fig. 3 and Table 2). It is of interest that activation of endothelin B receptors induces CREB phosphorylation and transcription of CREB target genes such as c-fos (47). Another gene of interest induced by CREB is adrenomedullin, known to be involved in tumorigenesis. Adrenomedullin is expressed in a variety of tumors where it aggravates several of the molecular and physiological features of malignant cells. It has been shown to be a mitogenic and survival factor for cancer cells and to prevent apoptosis. Adrenomedullin plays an important role in low oxygen tension environments, which is a typical feature of solid tumors. Under hypoxic conditions, adrenomedullin is up-regulated through a HIF-1-dependent pathway and acts as a potent angiogenic factor promoting neovascularization (48). Our findings show that adrenomedullin expression is also mediated in a CREB-dependent manner. We have demonstrated by DNA microarray and real-time PCR experiments that Cyr61, a member of the CCN family of genes (43), is up-regulated by CREB at hypoxia, probably through the putative CRE-like site at position -81 in the promoter region. This gene was found to be hypoxia inducible in malignant melanoma cells and controlled by activator protein 1 and HIF-1 α (44).

Additional genes relevant to tumor progression mediated by CREB revealed by the DNA array experiments include the following: the multifunctional cytoplasmic p62 (sequestosome1), overabundance of p62 protein in malignant breast tissue relative to normal breast tissue was shown recently (49); Galactin8 (Lgals8) that was found to modulate the behavior of several human tumors (50, 51); the ets variant gene 6, also known as the TEL oncogene, a transcription factor involved in several chromosomal translocations, t(12,21), common in childhood acute lymphoblastic leukemia, and the t(8,21) in acute myeloid leukemia; and the oncogene pim3 is a known transcriptional target of divergent EWS/ETS oncoproteins found in the Ewing's sarcoma family of tumors.

The genes discussed above, as well as many others shown in Table 2 and Fig. 3 as CREB targets, substantiate a potential major regulatory function for CREB in cancer. Other genes, involved in cell metabolism, transport, RNA processing, and stability, could be involved in cancerogenesis in an indirect way. It is worth mentioning the up-regulation of genes such as Herpud1 and Atf4, known to be involved in stress response (52, 53).

The results presented in this work link CREB to cellular responses to hypoxia in parallel to other proteins such as HIF. We demonstrated that CREB dramatically affects cellular functions such as enhanced growth, increased angiogenesis, and decreased apoptosis, which define the fate of a growing tumor.

ACKNOWLEDGMENTS

We thank the Arison family donation for the Center of DNA chips in Pediatric Oncology and Promega Corporation for the support in reagents to Dr. Honigman.

REFERENCES

1. Brindle, P., Linke, S., and Montminy, M. Analysis of a PK-A dependent activator in CREB reveals a new role for the CREM family of repressors. *Nature (Lond.)*, *364*: 821–824, 1993.
2. Quinn, P. G. Distinct activation domains within cAMP response element-binding protein (CREB) mediate basal and cAMP-stimulated transcription. *J. Biol. Chem.*, *268*: 16999–17009, 1993.
3. Goren, I., Tavor, E., Goldblum, A., and Honigman, A. Two Cystein residues in the DNA binding domain of CREB control binding to CRE and CREB mediated gene expression. *J. Mol. Biol.*, *313*: 695–709, 2001.
4. Montminy, M. R., Sevarino, K. A., Wagner, J. A., Mandel, G., and Goodman, R. H. Identification of a cyclic-AMP responsive element within the rat somatostatin gene. *Proc. Natl. Acad. Sci. USA*, *83*: 6682–6686, 1986.
5. Comb, M., Burnberg, N. C., Seascholtz, A., Herbert, E., and Goodman, H. M. A cyclic-AMP- and phorbol ester-inducible DNA element. *Nature (Lond.)*, *323*: 353–356, 1986.
6. Short, J. M., Wynshaw-Boris, A., Short, H. P., and Hanson, R. W. Characterization of the phosphoenolpyruvate carboxykinase (GTP) promoter-regulatory region. II. Identification of cAMP and glucocorticoid regulatory domains. *J. Biol. Chem.*, *261*: 9721–9726, 1986.
7. Benbrook, D. M., and Jones, N. C. Heterodimer formation between CREB and Jun proteins. *Oncogene*, *5*: 295–302, 1990.
8. Iannello, R. C., Young, J., Sumarsono, S., Tymms, M. J., Dahl, H. H., Gould, J., Hedger, M., and Kola, I. Regulation of Pdh-2 expression is mediated by proximal promoter sequences and CpG methylation. *Mol. Cell. Biol.*, *17*: 612–619, 1997.
9. Richards, J. P., Baechinger, P. H., Goodman, R. H., and Brennan, R. G. Analysis of the structural properties of cAMP-responsive element-binding protein (CREB) and phosphorylated CREB. *J. Biol. Chem.*, *271*: 13716–13723, 1996.
10. Hagiwara, M., Brindle, P., Harootyan, A., Armstrong, R., Rivier, J., Vale, W., Tsien, R., and Montminy, M. R. Coupling of hormonal stimulation and transcription via cyclic-AMP-responsive factor CREB is rate limited by nuclear entry of protein kinase A. *Mol. Cell. Biol.*, *13*: 4852–4859, 1993.
11. Chrivia, J. C., Kwok, R. P., Lamb, N., Hagiwara, M., Montminy, M. R., and Goodman, R. H. Phosphorylated CREB binds specifically to the nuclear protein CBP. *Nature (Lond.)*, *365*: 855–859, 1993.
12. Gonzales, G. A., and Montminy, M. R. Cyclic AMP stimulates somatostatin gene transcription by phosphorylation of CREB at serine-133. *Cell*, *59*: 675–680, 1989.
13. Andrisani, O. M. CREB mediated transcriptional control. *Crit. Rev. Eukaryotic Gene Exp.*, *9*: 19–32, 1999.
14. Sheng, M., Thompson, M. A., and Greenberg, M. E. CREB: a Ca(2+)-regulated transcription factor phosphorylated by calmodulin-dependent kinases. *Science (Wash. DC)*, *252*: 1427–1430, 1991.
15. Xing, J., Ginty, D. D., and Greenberg, M. E. Coupling of the RAS-MAPK pathway to gene activation by RSK2, a growth factor-regulated CREB kinase. *Science (Wash. DC)*, *273*: 959–963, 1996.
16. Mayr, B., and Montminy, M. Transcriptional regulation by the phosphorylation-dependent factor CREB. *Nat. Rev. Mol. Cell. Biol.*, *2*: 599–609, 2001.
17. Mayo, L. D., Kessler, K. M., Pincheira, R., Warren, R. S., and Donner, D. B. Vascular endothelial cell growth factor activates CRE binding protein by signaling through the KDR receptor tyrosine kinase. *J. Biol. Chem.*, *276*: 25184–25189, 2001.
18. Firth, J. D., Ebert, B. L., and Ratcliffe, P. J. Hypoxic regulation of Lactate dehydrogenase A. *J. Biol. Chem.*, *270*: 21021–21027, 1995.
19. Dong, Z., Nishiyama, J., Yi, X., Venkatachalam, M. A., Denton, M., Gu, S., Li, S., and Qiang, M. Gene promoter of apoptosis inhibitory protein IAP2: identification of enhancer element and activation by hypoxia. *Biochem. J.*, *364*: 413–421, 2002.
20. Freeland, K., Boxer, L. M., and Lachman, D. The cyclic AMP response element in the BCL2 promoter confers inducibility by hypoxia in neuronal cells. *Mol. Brain Res.*, *92*: 98–106, 2001.
21. Long, F., Schipani, E., Asahara, H., Kronenberg, H., and Montminy, M. The CREB family of activators is required for endochondral bone development. *Development (Camb.)*, *128*: 541–550, 2001.
22. Ionescu, A. M., Schwarz, E. M., Vinson, C., Puzas, J. E., Rosier, R., Reynolds, P. R., and O'Keefe, R. J. PTHrP modulates chondrocyte differentiation through AP-1 and CREB signaling. *J. Biol. Chem.*, *276*: 11639–11647, 2001.
23. Riccio, A., Ahn, S., Davenport, C. M., Blendy, L. A., and Ginty, D. D. Mediation by a CREB family transcription factor of NGF dependent survival of sympathetic neurons. *Science (Wash. DC)*, *286*: 2358–2361, 1999.
24. Bedogni, B., Pani, G., Colavitti, R., Riccio, A., Borrello, S., Murphy, M., Smith, R., Eboli, M. L., and Galeotti, T. Redox regulation of cAMP-responsive element-binding protein and induction of manganese superoxide dismutase in nerve growth factor-dependent cell survival. *J. Biol. Chem.*, *278*: 16510–16511, 2003.
25. Desdouets, C., Matesic, G., Molina, C. A., Foulkes, N. S., Sassone-Corsi, P., Brechet, C., and Sobczak-Thépot, J. Cell cycle regulation of cyclin A gene expression by the cyclic AMP-responsive transcription factors CREB and CREM. *Mol. Cell. Biol.*, *15*: 3301–3309, 1995.
26. Lee, R. J., Albanese, C., Stenger, R. J., Watanabe, G., Inghirami, G., Haines, G. K., III, Webster, M., Muller, W. J., Brugge, J. S., Davis, R. J., and Pestell, R. G. pp60(v-src) induction of cyclin D1 requires collaborative interactions between the extracellular signal-regulated kinase, p38, and Jun kinase pathways. A role for cAMP response element-binding protein and activating transcription factor-2 in pp60(v-src) signaling in breast cancer cells. *J. Biol. Chem.*, *274*: 7341–7350, 1999.
27. D'Amico, M., Hult, J., Amanatullah, D. F., Zafonte, B. T., Albanese, C., Bouzahzah, B., Fu, M., Augenlicht, L. H., Donehower, L. A., Takemaru, K., Moon, R. T., Davis, R., Lisanti, M. P., Shtutman, M., Zhurinsky, J., Ben-Ze'ev, A., Troussard, A. A., Dedhar, S., and Pestell, R. G. The integrin-linked kinase regulates the cyclin D1 gene

- through glycogen synthase kinase β and cAMP-responsive element-binding protein-dependent pathways. *J. Biol. Chem.*, 275: 32649–32657, 2000.
28. Park, Y. G., Nesterova, M., Agrawal, S., and Cho-Chung, Y. S. Dual blockade of cyclic AMP response element- (CRE) and AP-1-directed transcription by CRE-transcription factor decoy oligonucleotide. Gene-specific inhibition of tumor growth. *J. Biol. Chem.*, 274: 1573–1580, 1999.
 29. Cho, Y. S., Kim, M-K., Cheadle, C., Neary, C., Park, Y. G., Becker, K. G., and Cho-Chung, Y. S. A genomic-scale view of the CAMP response element-enhancer decoy: a tumor target-based genetic tool. *Proc. Natl. Acad. Sci., USA*, 99: 15626–15631, 2002.
 30. Rosenberg, D., Groussin, L., Bertagna, X., and Bertherat, J. cAMP pathway alterations from the cell surface to nucleus in adrenocortical tumors. *Endocr. Res.*, 28: 765–775, 2002.
 31. Rosenberg, D., Groussin, L., Julian, E., Perlemoine, K., Bertagna, X., and Bertherat, J. Role of the PKA-regulated transcription factor CREB in development and tumorigenesis of endocrine tissues. *Ann. N. Y. Acad. Sci.*, 968: 65–74, 2002.
 32. Jean, D., and Bar-Eli, M. Regulation of tumor growth and metastasis of human melanoma by the CREB transcription factor family. *Mol. Cell. Biochem.*, 212: 19–28, 2000.
 33. Jean, D., and Bar-Eli, M. Targeting the ATF-1/CREB transcription factors by signaling chain Fv fragment in human melanoma: potential modality for cancer therapy. *Crit. Rev. Immunol.*, 21: 275–286, 2001.
 34. Shaywitz, A. J., and Greenberg, M. E. CREB: a stimulus-induced transcription factor activated by a diverse array of extracellular signals. *Annu. Rev. Biochem.*, 68: 821–861, 1999.
 35. Honigman, A., Zeira, E., Ohana, P., Abramovitch, R., Tavor, E., Bar, I., *et al.* Imaging transgene expression in live animals. *Mol. Ther.*, 4: 239–249, 2001.
 36. Goren, I., Tavor, E., and Honigman, A. Gene regulation mediated by interaction between HTLV-1 promoter elements and transcription factors Tax and CREB. *Virology*, 256: 303–312, 1999.
 37. Affymetrix Technical Note2 “Fine Tuning Your Data Analysis.” Part Number 701138 rev2, 2001.
 38. Eisen, M. B., Spellman, P. T., Brown, P. O., and Botstein, Cluster analysis and display of genome-wide expression patterns. *Proc. Natl. Acad. Sci. USA.*, 95: 14863–14868, 1998.
 39. Abramovitch, R., Frenkiel, D., and Neeman, M. Analysis of subcutaneous angiogenesis by gradient echo magnetic resonance imaging. *Magn. Reson. Med.*, 39: 813–824, 1998.
 40. Abramovitch, R., Dafni, H., Smouha, E., Benjamin, L., and Neeman, M. *In vivo* prediction of vascular susceptibility to vascular endothelial growth factor withdrawal: magnetic resonance imaging of C6 rat glioma in nude mice. *Cancer Res.*, 59: 5012–5016, 1999.
 41. Harris, A. L. Hypoxia-A key regulatory factor in tumour growth. *Nat. Rev. Cancer*, 2: 38–47, 2001.
 42. Bracken, C. P., Whitelaw, M. L., and Peet, D. J. The hypoxia-inducible factors: key transcriptional regulators of hypoxia responses. *Cell Mol. Life Sci.*, 60: 1376–1393, 2003.
 43. Sawai, K., Mori, K., Mukoyama, M., Sugawara, A., Suganami, T., Koshikawa, M., Yahata, K., Makino, H., Nagae, T., Fujinaga, Y., Yokoi, H., Yoshioka, T., Yoshimoto, A., Tanaka, I., and Nakao, K. Angiogenic protein Cyr61 is expressed by podocytes in anti-Thy-1 glomerulonephritis. *J. Am. Soc. Nephrol.*, 14: 1154–1163, 2003.
 44. Kunz, M., Moeller, S., Koczan, D., Loenz, P., Wenger, RH., Glocker, MO., Thiesen H., Gross, G., and Ibrahim, S. M., Mechanism of hypoxic gene regulation of angiogenesis factor Cyr61 in melanoma cells. *J. Biol. Chem.*, 278: 45651–45660, 2003.
 45. Cho-Chung, Y. S., Park, Y. G., Nesterova, M., Lee, Y. N., and Cho, Y. S. CRE-decoy oligonucleotides inhibition of gene expression and tumor growth. *Mol. Cell. Biochem.*, 212: 29–34, 2000.
 46. Grant, K., Loizidou, M., and Taylor, I. Endothelin-1: a multifunctional molecule in cancer. *Br. J. Cancer*, 88: 163–166, 2003.
 47. Schinelli, S., Zanassi, P., Paolillo, M., Wang, H., Feliciello, A., and Gallo, V. Stimulation of endothelin B receptors in astrocytes induces cAMP response element-binding protein phosphorylation and c-fos expression via multiple mitogen-activated protein kinase signaling pathways. *J. Neurosci.*, 21: 8842–8853, 2001.
 48. Zudaier, E., Martinez, A., and Cuttita, F. Adrenomedullin and cancer. *Regul. Pept.*, 112: 175–183, 2003.
 49. Thompson, H. G., Harris, J. W., Wold, B. J., Lin, F., and Brody, J. P. p62 overexpression in breast tumors and regulation by prostate-derived Ets factor in breast cancer cells. *Oncogene*, 22: 2322–2333, 2003.
 50. Danguy, A., Camb, Y. I., and Kiss, R. Galectins and cancer. *Biochim. Biophys. Acta*, 1572: 285–293, 2002.
 51. Levy, Y., Ronen, D., Bershadsky, A. D., and Zick, Y. Sustained induction of ERK, protein kinase B, and p70 S6 kinase regulates cell spreading and formation of F-actin microspikes upon ligation of integrins by galectin-8, a mammalian lectin. *J. Biol. Chem.*, 278: 14533–14542, 2003.
 52. Segawa, T., Nau, M. E., Xu, L. L., Chilukuri, R. N., Makarem, M., Zhang, W., Petrovics, G., Sesterhenn, I. A., McLeod, D. G., Moul, J. W., Vahey, M., and Srivastava, S. Androgen-induced expression of endoplasmic reticulum (ER) stress response genes in prostate cancer cells. *Oncogene*, 21: 8749–8758, 2002.
 53. Rutkowski, D. T., and Kaufman, R. J. All roads lead to ATF4. *Dev. Cell*, 4: 442–444, 2003.